DETECTION AND DIFFERENTIATION OF SELECTED RICE DISEASES USING HYPERSPECTRAL DATA

Jean Rochielle F. Mirandilla (1)(2), Enrico C. Paringit (1)

[1] University of the Philippines, Diliman, Quezon City, Philippines

[2] Philippine Rice Research Institute, Batang, Ligao City, Albay, Philippines
Email: jeanrochiellemirandilla@gmail.com; paringit@gmail.com

ABSTRACT: Pests and diseases contributed to declining productivity in rice production. Monitoring the plant health and early detection of the disease are essential to facilitate effective management practices, decrease disease spread, and minimize yield loss. Remote sensing (RS) techniques such as use of hyperspectral data can provide timely information on spatial variability of pest and disease damage over a large area. Hyperspectral data is composed of contiguous spectral bands which allows improved analysis of specific compounds, molecular interactions, crop stress, and biophysical or biochemical characteristics related to plant status.

This study aimed to use hyperspectral data to detect and differentiate the three-major diseases in the Philippines. Reflectance spectra of rice leaves infected with the three pathogens rice tungro virus, *Xanthomonas oryzae pv. oryzae* and *Magnaporthe oryzae* causing rice tungro disease, bacterial leaf blight (BLB), and blast, respectively, were recorded repeatedly from the inoculation to the late stages of the diseases. Hyperspectral data were analyzed using different data analysis such as ANOVA, cluster analysis and spectral features. The IRRI Standard Evaluation System (SES) for rice were used for visual assessment to determine the degree of severity and incidence of the disease.

Based on the results, spectral reflectance of rice was affected by each disease in a characteristic way resulting to different spectral signature. Reflectance differences, sensitivity, and first order derivatives differed depending on the disease and the developmental stage of the diseases. Red and red-edge ranges are the most sensitive to the three diseases. Moreover, near-infrared wavelengths decreased as the disease progress. In addition, yellow-orange range (550 – 620 nm) is very sensitive during the early stage of tungro. The results of cluster analysis showed that Tungro can be detected in 10% or less height reduction and no distinct yellow to yellow orange leaf discoloration while BLB can be detected when affected area is 5% or less. On the other hand, blast was detected in its late stage, more than 75% of leaf area are affected. This study illustrates the potential use of hyperspectral data in detecting tungro disease, bacterial leaf blight (BLB), and blast in rice.

1. INTRODUCTION

Rice provides the main source of energy for Filipinos where an average family requires 37% of rice and its products daily (Ponce and Inocencio, 2017). In 2017, Philippine Statistics Authority reports that the average yield of palay is 4.00 tons/ha, 4.41 tons/ha in irrigated and 3.11 in rainfed rice areas (PSA, 2018). Department of Agriculture (DA) said that the country reached 96% rice self-sufficiency, however, it is still not enough to sustain the need of all Filipinos.

Damage caused by pests and diseases plays a significant role in crop losses throughout the world. The losses in crop yield due to pathogen infections, animals and weeds range between 20% and 40% (Savary, et al, 2012) of agricultural production, yield loss for rice range at 30% globally (Savary et al., 2019). To minimize these losses on agricultural production, monitoring and early detection of pests and diseases are necessary to decrease disease spread and facilitate effective management practices.

Information about the incidence and severity of the disease is particularly important for rapid management decisions, especially disease occurrence is closely related to yield loss. Traditionally, pest and disease assessment is done by visual method i.e. observing symptoms and rating the incidence. Recent detection and identification of diseases and disease causal organism can be done through direct and indirect methods. Direct detection includes molecular and serological methods that can be used for high-throughput analysis when large numbers of samples need to be analyzed. The disease-causing pathogens (i.e. bacteria, fungi, and viruses) are directly detected in these methods to provide accurate identification of the disease and pathogen. In contrast, indirect methods identify the plant diseases through various parameters such as morphological change, temperature change, transpiration rate change and volatile organic compounds released by infected plants (Fang and Ramasamy, 2015). However, direct

traditional and innovative methods to detect and identify plant diseases are laborious and very costly.

Remote sensing (RS) techniques, as an indirect method, are based on the assumption that the stress affects the physical structure and photosynthesis of the plants thus influencing the absorption of light energy. In addition, RS can give a synoptic view of the area in a non-destructive and noninvasive way that could effectively provide timely information on spatial variability of pest damage (Prabkahar, et al, 2011). Measurements in remote sensing can be acquired by portable instruments such as handheld spectroradiometers. These measurements are processed and analyzed to retrieve information on the object observed. The optical sensors provide detailed information based on different electromagnetic spectra and thus, enable prediction of the plant health (Martinelli, et al, 2013).

Several studies have been conducted to assess the use of hyperspectral data in detection of various diseases in rice such as panicle blast, bacterial leaf blight (blb), brown spot and injuries from brown planthopper (BPH) in a certain rice stage (Kobayashi, et al, 2001, Kobayashi, et al, 2015, Prasannakumar, et al, 2014). These pests and diseases exhibit different symptoms, levels of incidence and yield reduction in rice. Kobayashi et. al, evaluated the use of airborne hyperspectral imagery to measure the severity of panicle blast in field crops. Based on the results, at the dough stage, there are two band ratios that exhibited significant correlations with disease incidence (R498 to 515/R700 to 717 and R472 to 489/R558 to 575) (Kobayashi, et al, 2015). In addition, four correlations sensitive wavelengths at 764, 961, 1201 and 1664 can be depicted the relation of between BPH stress on the rice crop and plant reflectance (Prasannakumar, et al, 2014). Different statistical methods were used to estimate and define the severity of rice brown spot at the leaf level. Results revealed that multiple stepwise linear regressions and partial least-square regression could efficiently estimate disease severity. Moreover, based on the results of Singh et. al, 2012 in the use of hyperspectral data, notable differences in healthy and blb infected rice plants were noticed in 770–860 nm and 920–1050 nm. The hyperspectral data were collected in the different disease incidence at 75 days after sowing (Singh, et al, 2012).

Hyperspectral data have been successfully used to distinguish between healthy and diseased plant. Since the disease symptoms can be seen in the leaves, there is a possibility that it can be detected using remote sensing. This is possible because healthy and diseased plants reflect energy differently. The common rice pests and diseases that cause extensive damage and losses in rice-producing areas in the Philippines are brown planthopper (BPH), bacterial leaf blight, rice blast, sheath blight, and rice tungro. As such, eighteen provinces in the country were affected by BPH in 2017 and nine provinces in 2015 (Fernandez R., 2017). In September 2016, Western Visayas reported the occurrence of rice blast and sheath blight affecting over 3,000 ha of rice lands in the region (Herriman R., 2016). Hence, this study will use hyperspectral data to detect and differentiate the three major rice diseases in the Philippines - blast, bacterial leaf blight (BLB), rice tungro disease that are caused by different pathogens, fungi, bacteria, and virus, respectively. Specific objectives were to (1) Understand the difference of spectral responses among the three-major pest and diseases and identify the spectral regions in which rice reflectance was affected by these pests and disease; and (2) Identify efficient spectral features for differentiating the three stressors.

2. METHODOLOGY

2.1 Establishment of the study

The experiment was established in PhilRice Central Experiment Station in Muñoz, Nueva Ecija screenhouse and experimental field. Both blast and tungro set-up were planted inside the screenhouse to prevent the spreading of the disease in the experiment area. While, Bacterial Leaf Blight (BLB) was established in the experimental area.

Susceptible and resistant varieties were inoculated using the National Cooperative Testing (NCT) protocols for disease inoculation. Glh introduction, clipping method and spreader rows techniques were used for inculation of tungro, blb and blast, respectively. Inoculated and uninoculated plants were planted in plots with three replications. Uninoculated plants served as the control for each disease. Plants were inoculated during the most critical stage of rice plant for the disease infection. Blast and tungro were inoculated at seedling while blb at maximum tillering.

2.2 Data acquisition

2.2.1 Spectral Measurements

Spectral responses were measured using Ocean Optics USB4000-VIS-NIR-ES spectrometer in leaf level. Ocean Optics USB4000-VIS-NIR-ES spectrometer is a miniature spectrometer pre-configured for general visible and near-IR measurements. Five (5) selected plants per plot and replication were selected to measure the spectral responses. These sample plants were measured almost daily before and after the introduction of the inoculum to the plants until the diseases were reach International Rice Research Institute Standard Evaluation System for Rice (IRRI SES)

score of 9 (Table 1).

2.2.2 Agronomic parameters and weather data

Agronomic parameters such as LAI and plant height were measured every week. LAI was measured using AccuPAR LP-80 ceptometer, in 3 replicates within each plot with at least 2 plants away from each other and bunds. Meanwhile, plant height was measured once a week in 5 sampling plants per plot. To detect the disease infection in the rice plants, visual symptoms of the 3 diseases were assessed using SES. SES uses scale that divides total range of possible phenotypic expressions in rice to have a common standard for evaluation. Table 1 shows the different SES scale for determining the incidence or severity of 3 selected rice diseases.

Table 1. IRRI Standard Evaluation System scale for tungro, BLB and blast disease

Scale	Tungro	BLB (field)	Blast (nursery)
0			No lesions observed
1	No symptom observed	1-5%	Small brown specks of pin-point size or larger brown specks without sporulating center
3	1-10% height reduction, no distinct yellow to yellow orange leaf discoloration	6-12%	Lesion type is the same as in scale 2, but a significant number of lesions are on the upper leaves
5	11-30% height reduction, no distinct yellow to yellow orange leaf discoloration	13-25%	Typical blast lesions infecting 4-10% of the leaf area
7	31-50% height reduction, with distinct yellow to yellow orange leaf discoloration	26-50%	Typical blast lesions infection 26-50% of the leaf area
9	More than 50% height reduction, with distinct yellow to yellow orange discoloration	51-100%	More than 75% leaf area affected

2.3 Data analysis

2.3.1 Data preparation

All the saved text file containing the nominal radiance and irradiance were copied in Microsoft Excel. Average readings for each white reference panel and each target object were computed. Reflectance of each target objects was computed using the formula below.

(Equation 1)

$$Ref(\lambda) = \frac{E(\lambda)_{sample} - E(\lambda)_{dark}}{E(\lambda)_{white} - E(\lambda)_{dark}}$$

Where $E(\lambda)_{sample}$ is the nominal radiance and $E(\lambda)_{white}$ is irradiance measured by the white panel and $E(\lambda)_{dark}$ by the dark object.

The spectral data was smoothen using Savitzky–Golay smoothing method. It is a digital filter that can be applied to a set of digital data points for the purpose of smoothing the data, that is, to increase the signal-to-noise ratio without greatly distorting the signal. 5 weighting coefficients was used as a parameter. The wavelengths from 400 nm to 850 nm were used in generating the spectral library. Wavelengths from 345 – 400 and >850 nm were omitted since the noise was high.

As the leaf spectra of RTV, blast and BLB were collected from different cultivars, a spectral normalization was implemented at first to adjust the spectral data from different groups to an identical baseline. This procedure facilitates spectral comparison between different stressors (Zhang et al., 2012). The benefit of such a normalization is the suppression of illumination differences. The formula used is as follows:

(Equation 2)

$$Ref(\lambda)_{norm} = \frac{Ref(\lambda)_i}{\frac{1}{n}(\sum_{i=1}^{n} Ref(\lambda)_i)}$$

Where, $R(\lambda)_{norm}$ is the normalized reflectance for band i; $R(\lambda)_i$ is the original reflectance of the band; n is the total effective number of bands.

2.3.2 Ratio Spectra (Sensitivity)

Ratio spectra (sensitivity) are ways to enhance differences between spectral signatures and determine sensitive and significant wavelengths for a disease (Yuan et al., 2014). The ratio curve reflects both change direction (increase or decrease) and change magnitude of reflectance, it can be treated as a spectral signature of a specific stressor. The formulas were as follows:

(Equation 3)

$$Ratio_{(stress)} = \frac{Ref_{(unhealthy)}}{Ref_{(healthy)}}$$

Where, $Ref_{(unhealthy)}$ is the average reflectance of the stressed samples; $Ref_{(healthy)}$ is the average reflectance of corresponding healthy samples.

2.3.3 Spectral library and Cluster analysis

Using ENVI 4.7 spectral library builder, all the spectral measurements were databased in different spectral libraries. The spectral libraries were resampled to SentinelA. Sentinel 2 is a European wide-swath, high-resolution, multi-spectral imaging mission. (https://sentinel.esa.int/). Resampling is used to either the response of a known instrument the wavelengths of a specific image input file. Cluster analysis is an unsupervised classification technique to group similar observations into a number of clusters based on the observed values of several variables for each individual. Hierarchal clustering is tree-based representation of the observations which is called a dendrogram. The study used agglomerative method or Agglomerative Nesting (AGNES), which works in a bottom-up manner (Hartigan, J. A., 2015). The two 'closest' (most similar) clusters are then combined and this is done repeatedly until all subjects are in one cluster. The analysis was performed to determine the possible earliest date to detect the 3 diseases by grouping the dates with similar spectral values. The values used for the analysis were from the resampled reflectance from Sentinel 2.

2.3.4 Statistical analysis

Using the different spectral ranges as group, statistical analyses were performed using the IBM SPSS. Data from repeated measures was analyzed using a general linear model and the Bonferroni correction to determine statistically significant differences (p = 0.01; p = 0.05). Bonferroni test is a multiple-comparison post-hoc correction used in performing many independent or dependent statistical tests at the same time (Weisstein, Eric). Data were analyzed by analysis of variance (ANOVA).

3. RESULTS AND DISCUSSION

3.1 Disease progress in leaf

Tungro, BLB and blast have different causal pathogens, virus, bacteria and fungi, respectively. Depending on the pathogens, the 3 diseases of rice were characterized by disease-specific symptoms. Inoculated plants were first colonized without symptoms, after a latent period typical symptom appeared. Figure 1 shows the infected leaves with a 9-score scale of 3 different diseases.
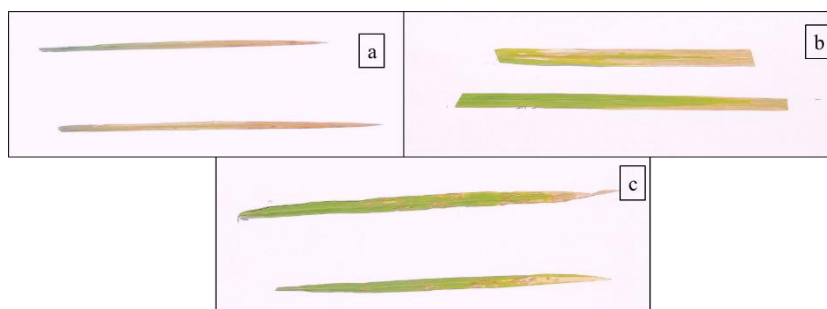

Figure 1. Infected leaves of (a) tungro, (b) BLB, and (c) blast

Spectral measurements were done daily except for days that were too cloudy and rainy. As shown in Table 3, 11 dates were selected and used in the analysis of the study. The dates were chosen based on its corresponding SES scale and appearance of the visual symptoms in the leaves of the plants.

Table 3. Different dates of spectral measurement of the 3 diseases with corresponding SES scale score.

Date	Tungro			BLB			Blast		
	Date	SES Scale	DAI	Date	SES Scale	DAI	Date	SES Scale	DAI
1	01/18/2018	1	9	03/16/2018	0	0	03/25/2018	0	4
2	01/24/2018	1	15	03/22/2018	0	0	03/28/2018	1	7
3	01/25/2018	1	16	03/27/2018	1	4	03/29/2018	1	8
4	01/28/2018	1	19	03/28/2018	1	5	03/30/2018	1	9
5	01/31/2018	3	22	03/29/2018	3	6	04/03/2018	3	13
6	02/01/2018	5	23	03/30/2018	5	7	04/05/2018	5	15
7	02/03/2018	5	25	04/03/2018	5	11	04/06/2018	5	16
8	02/04/2018	5	26	04/04/2018	7	12	04/12/2018	7	22
9	02/09/2018	7	31	04/05/2018	7	13	04/18/2018	7	28
10	02/14/2018	9	36	04/06/2018	7	14	04/25/2018	9	35
11	02/16/2018	9	38	04/12/2018	9	20	04/27/2018	9	37

*Days after inoculation (DAI)

3.2 Spectral reflectance

3.2.1 Leaf reflectance

Tungro

Rice tungro virus disease main symptoms are stunting and yellow to orange discoloration of the leaves (Azzam and Chancellor, 2002). With these, changes can be seen in the spectral signatures of leaves infected by tungro. The first visible symptom was seen in 22 DAI (Date 5). Figure 2 shows the differences among the test varieties in response to tungro infection. As the disease progress, reflectance between 400 to 500 nm and 600 to 700 nm of the susceptible variety increased compared to the other varieties. In contrast, NIR region (700 – 850 nm) reflectance decreased. The slope at the red edge position between visible and NIR became less steep and shifted to the left.Based on -the results of ANOVA, all spectral reflectance of susceptible variety was significantly different from the other varieties except in the blue range (Figure 3a). All the test varieties in green range (520-580 nm) were in decreasing trend as the rice plant grows and the infection progress. However, the susceptible variety had higher reflectance values compared to the other varieties. It was observed that both red and red-edge range reflectance of the susceptible variety were increasing as the disease progress. This can be attributed to the strong reflectance of pigments in the red - red-edge ranges. Pigments such as chlorophyll a & b, and carotenoids decrease as stress introduced to the plants (Subbarao et al, 1979). In contrast, NIR reflectance decreased gradually as the disease incidence increased. The absorptance in this region is dominated by internal leaf structure. Reflectance, generally high in this regiondue to refractive discontinuities between intercellular air spaces and cell walls (Croft and Chen, 2018). However, during the disease pathogenesis, these leaf structures were damaged by the disease making the reflectance decrease.
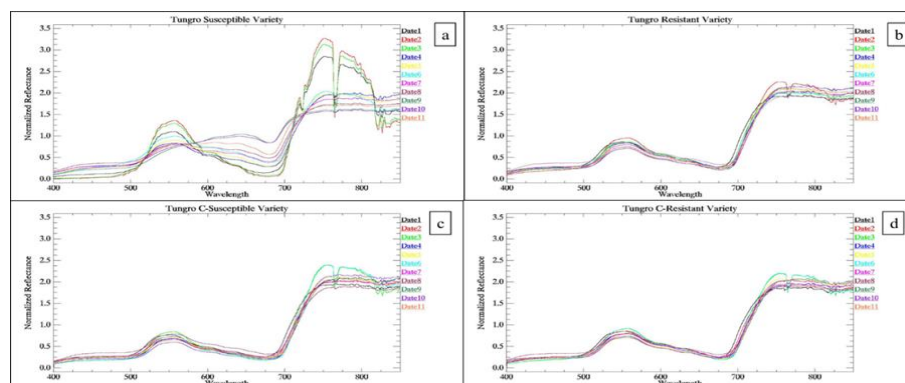

Figure 2. Leaf spectral reflectance among different varieties (a) susceptible, (b) resistant, (c) susceptible control, (d) resistant control in response to Tungro inoculation
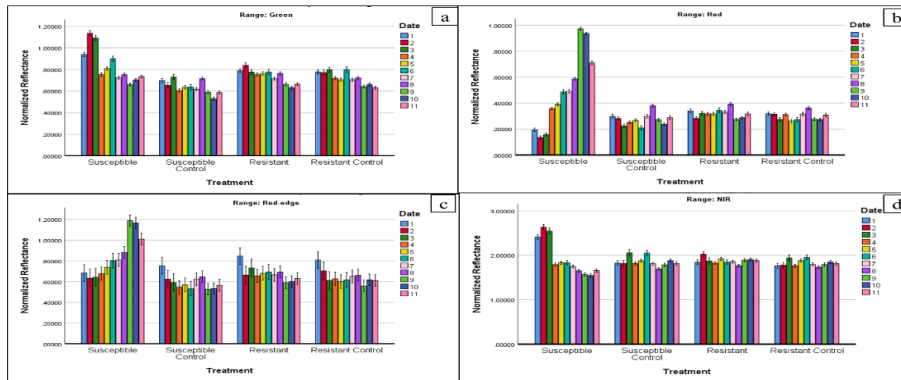
Figure 3. Reflectance ranges (a) green, (b) red, (c) red-edge, and (d) NIR of entries in response to Tungro.

Bacterial Leaf Blight

Yellow - orange stripes, the early symptoms of the blb, were observed in the clipped tips at 4 DAI. After 20 days of inoculation, the scale reached the 9 scale in SES, more than 50% of the leaf area is infected by BLB.

Spectral measurements for BLB set-up started in early tillering until flowering. As shown in Figure 4, blue range (400 – 500nm) reflectance was not affected by the infection. However, there was an increase in 450 – 500 nm when the disease reached 51% infection (Date11). In addition, an increase of reflectance in the wavelength range of 550 - 680 nm can be seen compared to the other treatments. The difference of NIR reflectance in susceptible variety from the first date to the last date is bigger than the other treatments. Figure 5 shows the different response of each reflectance range to BLB inoculation. Susceptible variety was significantly different across the dates and among the other varieties. Blue, red, and red-edge ranges reflectance of susceptible variety are higher than among the control and resistant varieties and increased as the disease progress in the plant. In contrast, NIR reflectance values were lower in susceptible variety compared to other varieties especially during the late stages of the disease. Leaf tissues are tend to be destroyed by diseases as a result multiple scattering in the leaf is weaker. This lead to lower the NIR reflectance in non-healthy leaf than the healthy leaf (Yuam et al, 2014).
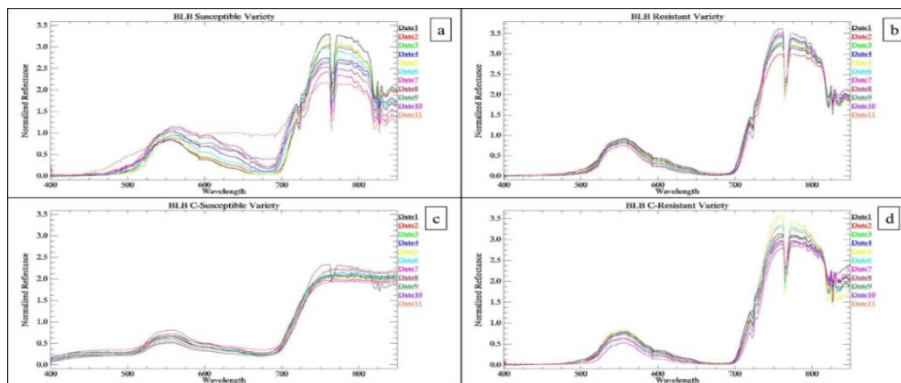

Figure 4. Leaf spectral reflectance among different varieties (a) susceptible, (b) resistant, (c) susceptible control, (d) resistant control in response to BLB inoculation
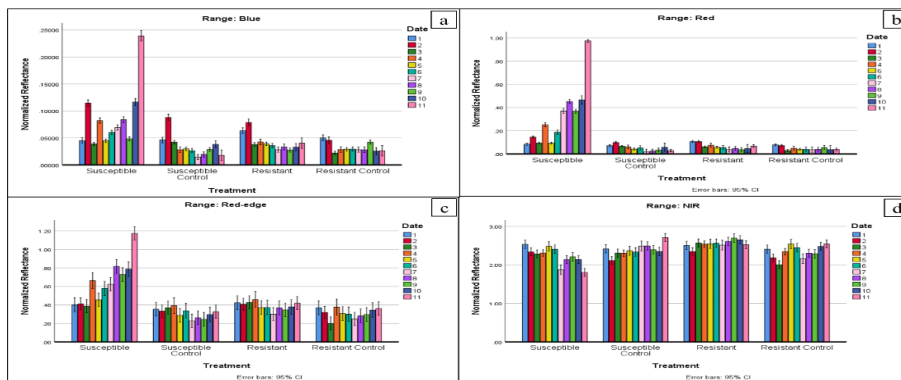

Figure 5. Reflectance ranges (a) blue, (b) red, (c) red-edge, and (d) NIR of different entries in response to blb.

Singh et al. (2012) also studied the use of hyperspectral data to detect BLB at the different disease infection. Based on the results, there are notable differences between healthy and diseased rice plants in NIR region (770 – 860 nm and 920 – 1050 nm). This is similar to the results of this study, NIR region (720 – 850 nm) is sensitive to BLB especially in later stages of the disease. However, red - red-edge region (550 - 680 nm) was the most sensitive region to BLB infection.

Blast

First symptoms of blast appeared in susceptible variety 7 DAT. Small brown specks of pin-point size or larger brown specks were observed in the leaves. The disease progressed to more than 75% leaf area affected in 37 DAT. Changes in reflectance spectra were comparatively low for blast compared to tungro and blast (Figure 6). This can be due to symptom is initially appeared as pin-point sized brown specks that is scattered to the leaves. The lesions will become large elliptical or spindle-shaped with red to brownish or necrotic border that spread in the larger area of the leaf. Same reaction was seen in tungro and blb infection that reflectance in 600 – 700nm increased as the disease becomes severe. In addition, the reflectance in the NIR region (720 – 850nm) decreased during the late stages of the disease. More changes in the spectra were seen in the late stage of blast as the lesions were spread in the leaves and started to wilt and die. Similar to tungro and BLB, blast spectral ranges in susceptible variety were significantly different across the dates and among the different varieties (Figure 7). It was observed that blue, red and red-edge reflectance increased as the disease incidence increased. These ranges are very sensitive to stress since the pigments' absorption bands are mostly located in these ranges. It was also observed that NIR reflectance is slowly decreasing as the disease progress.
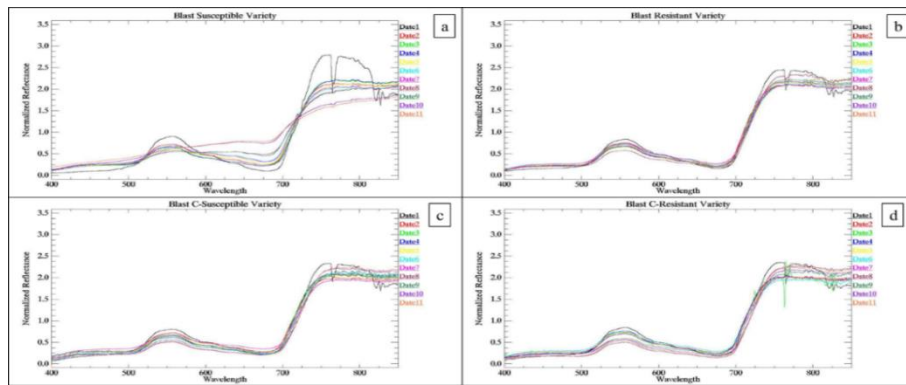

Figure 6. Leaf spectral reflectance among different varieties (a) susceptible, (b) resistant, (c) susceptible control, (d) resistant control in response to blast inoculation
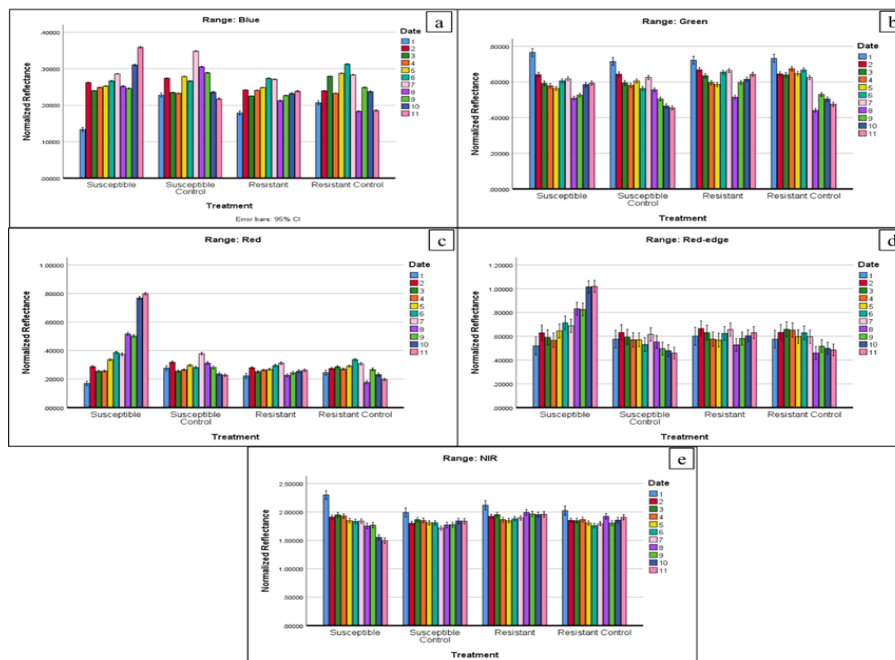

Figure 7. Reflectance ranges (a) blue, (b) green, (c) red, (d) red-edge, and (e) NIR of different entries in response to blb.

4.3 First order derivatives

Based on the first order derivatives shown in Figure 8, there are differences between the susceptible variety and susceptible control among the three diseases. In Figure 8a and 8c, tungro and blast susceptible variety have a shift in the wavelength range 700 – 750 nm. The first order derivative values become lower as the disease progress in the red-edge to NIR ranges. The red-edge region covers the wavelength range between red band absorption to the NIR shoulder (690–750 nm) which have a sharp increase in reflectance, in healthy plants. It features the transition from visible range strong absorption by leaf chlorophyll to the structural dominated reflectance in the NIR. This inflection point has been identified sensitive to changes in chlorophyll content (Croft & Chen, 2018).

In contrary, BLB has a very narrow shift in 680 – 700 nm range. It was observed that the values increased as the severity of the disease increased (Figure 8b). It was also observed that there is a strong absorption band between 760 – 770 nm in all the varieties. However, it disappeared in blast as the disease severity increased.
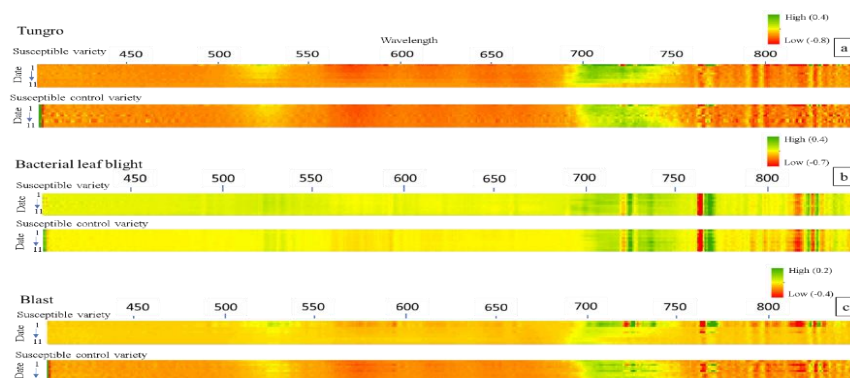

Figure 8. First order derivative reflectance among the selected rice disease in 400 – 850nm wavelengths

4.4 Cluster analysis

Cluster analysis was performed to determine the earliest date to detect the 3 diseases. As shown in Figure 9, different dates were grouped based on their similarities in resampled reflectance to the Sentinel 2. The highlighted clusters were dates that the rice infected plants were detected. Results of cluster analysis showed that tungro can be detected starting from the date 5, 21 days after the inoculation. The plants showed 1-10% height reduction, no distinct yellow to yellow orange leaf discoloration. In contrary, BLB can be detected starting date 4, 5 DAI, which had a SES score of 3 or 1-5% disease incidence. It can be seen in Figure 9b as the date 4 to date 11 were clustered compared from the other varieties' dates. However, date 5 can be observed that it is not included in the cluster, this can be explained by the low solar radiation during the data collection. Low solar radiation can lower the spectral reflectance as the sunlight is the only source of the light for measurement. Detection of blast started during the late stages of the disease development, 35 DAI, a SES score of 9 which means more than 75% of leaf area are affected. Late detection of blast can be explained by its symptom (Figure 9c). Early infection of blast has small lesions and occupy small area in the leaf making it hard to detect during early on-set of the disease (IRRI SES).

Figure 9. Hierarchal cluster analysis of resampled spectra to detect earliest date of diseases (a) tungro, (b) BLB, and (c) blast.

8

4.5 Difference and Sensitivity

Figure 10 shows the sensitivity of the three diseases susceptible variety. Susceptible variety is very sensitive to tungro infection as seen in Figure 2a. Blue range (450 – 550 nm) reflectance is a little unstable but generally it decreased as the disease progress. It was observed that yellow – orange range (550 – 620 nm) became sensitive in early stages of the disease but decreased in late stages. The sensitivity in this range can be attributed to the symptom exhibited by tungro infection, leaves have a distinct yellow to yellow orange color then turns brown as the leaves died in late stages. While, there was an increase of reflectance in the red-red edge range (640 – 720 nm). Green and red-red edge ranges are sensitive in both BLB (Figure 10b) and blast (Figure 10c) infection but they differ in number of sensitive wavelengths. Blast susceptible variety had more sensitive wavelengths than BLB, 600 – 740 nm and 625 – 725 nm, respectively. The three diseases are sensitive in red-red edge ranges. These ranges have been identified sensitive to changes in chlorophyll content of the plant especially the red edge region. Chlorophyll and anthocyanin are reflecting strongly in red wavelengths (Croft and Chen, 2018).
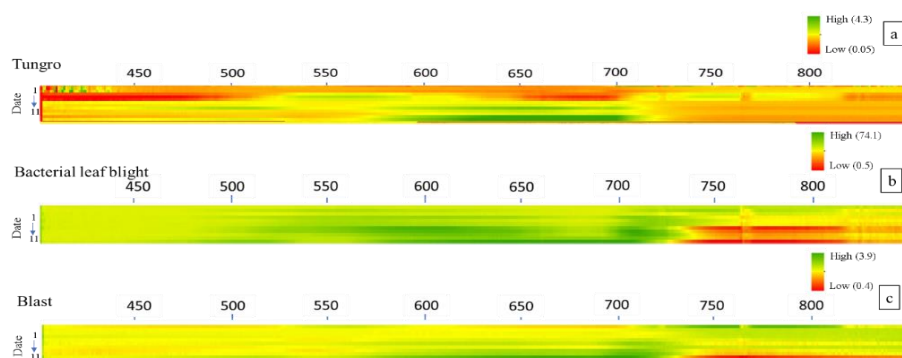

Figure 10. Sensitivity of susceptible variety in response to selected diseases

4. Conclusion and Recommendation

Reflectance spectra of rice leaves infected with the three pathogens rice tungro virus, Xanthomonas oryzae pv. oryzae and Magnaporthe oryzae causing rice tungro disease, bacterial leaf blight (BLB), and blast, respectively, were affected by each disease resulting in different spectral signature.

Based on the results, red and red-edge ranges were the most sensitive to the three diseases. The reflectance is increasing in both ranges as the disease incidence and severity increases. This can be attributed to the strong reflectance of pigments in these ranges. Subbarao et al., et al., 1979 stated that the pigments related to photosynthesis i.e. chlorophyll a & b, carotenoids and anthocyanin were destroyed during the disease infection. Moreover, red-edge marks the transition from strong absorption by leaf chlorophyll in the visible range to structural dominated reflectance in the NIR. Diseases infection in plants shifts the position of the red-edge and lower the steepness of the red-edge slope.

In addition, NIR reflectance decreases in all the diseases as the disease progress. The difference of NIR reflectance between healthy and unhealthy plants can be seen in later stages of the diseases. According to Croft and Chen in 2018, since, there are no strong absorption features in the NIR (>700nm). NIR reflectance is controlled by the ratio of mesophyll cell surface to intercellular air spaces, due to refractive discontinuities between intercellular air spaces and cell walls which is destroyed in later stage of the disease and senescence.

Reflectance sensitivity and first order derivatives (FOD) showed the differences of each disease. Based on first order derivatives values, there were differences between susceptible and susceptible control variety in tungro and blast infection. The values became lower as the disease progress in the red-edge to NIR ranges (700 – 750 nm) that caused a shift in wavelength range. No changes were observed in the FOD values in blb infected plants. Strong absorption bands were observed in the wavelengths between 760 – 770 nm in all the varieties. However, it disappeared in tungro and blast as the disease severity increased.

Reflectance sensitivity showed the changes of the significant wavelengths for the 3 diseases over time. It was observed that the yellow-orange range (550 – 620 nm) was very sensitive to tungro during the early stage of the disease. The sensitivity in this range can be attributed to the symptom exhibited by tungro infection, leaves have a distinct yellow to yellow orange color then turns brown in late stages. All the three diseases were sensitive in red and red-edge ranges; however, different number of wavelengths were observed. Tungro was sensitive in 640 – 720 nm compared to blast and blb that were sensitive in wavelengths 630 – 725 nm and 600 – 740 nm, respectively.

Cluster analysis was used to detect the earliest stages of the 3 diseases as the dates with similar values were grouped together. Based on the results, tungro and blb can effectively detect in the early stages of the diseases. Tungro can be detected when the plants were in less than 10% height reduction and no distinct yellow to yellow orange leaf

discoloration. In contrast, blb was detected 5 DAI in which area affected was less than 5%. Blast was detected in late stages when more than 75% of the leaf area were already affected. The late detection can be accounted that blast infection early symptoms were small lesions and occupy small area in the leaf (IRRI SES).

The study analysis is limited to ANOVA for repeated measures and independent t-test to differentiate the test varieties and 3 diseases. Hence, other techniques such as discriminant analysis and similarity index should be explored in order to possibly enhance the differentiation of the three diseases. In this study, the 3 diseases were detected and monitored by assessing visual symptoms of each disease and no actual detection of the pathogen was done. Therefore, to further establish the strong relationship between the remote sensing study and disease progression, it is recommended to perform direct analyses such as serological methods. Direct analyses can give the exact pathogen affect the plant.

5. References

Croft, H., & Chen, J. M. (2018). Leaf Pigment Content. Comprehensive Remote Sensing, 117–142. doi:10.1016/b978-0-12-409548-9.10547-0

Hartigan, J. (2015) Statistical Clustering. International Encyclopedia of the Social & Behavioral Sciences, 2nd edition, Volume 23. doi.org/10.1016/B978-0-08-097086-8.42176-8

Kobayashi, T., Kanda, E., Kitada, K., Ishiguro, K., Torigoe, Y., (2001). Detection of rice panicle blast with multispectral radiometer and the potential of using airborne multispectral scanners. Phytopathology 91 (3), 316–323.

Kobayashi, T., Kanda, E., Kitada, K., Ishiguro, K., Torigoe, Y., (2016). Assessment of Rice Panicle Blast Disease Using Airborne Hyperspectral Imagery. The Open Agriculture Journal, 2016, 10, 28-34

Fang, Yi, Ramaraja P. Ramasamy (2015). Current and Prospective Methods for Plant Disease Detection. Biosensors 2015, 4, 537-561; doi:10.3390/bios5030537

Fernandez R. (2017). Destructive rice pest reemerges in Philippines. The Philippine Star. November 18, 2017. https://www.philstar.com/business/agriculture/2017/11/18/1760241/destructive-rice-pest-reemerges-philippines

Herriman R. (2016). Rice blast, sheath blight threatens Iloilo rice crops. Outbreak News Today. Sept 10, 2016. http://outbreaknewstoday.com/rice-blast-sheath-blight-threaten-iloilo-rice-crops-44115/http://outbreaknewstoday.com/rice-blast-sheath-blight-threaten-iloilo-rice-crops-44115/

Philippine Statistics Authority (PSA), (2018). Selected Statistics on Agriculture 2018. ISSN-2012-0362 Retrieved from https://psa.gov.ph.

Ponce, E. Inocencio A., (2017) Toward a More Resilient and Competitive Philippine Rice Industry: Lessons from the Past Three Decades. Retrieved from IRRI website: https://www.irri.org/resources/publications/books/toward-a-more-resilient-and-competitive-philippine-rice-industry-lesson-from-the-past-three-decades

Prabkahar, M, Prasad YG, Rao MN, (2011). Remote sensing of biotic stress in crop plants and its applications for pest management. In: Crop Stress and its Management: Perspectives and Strategies, B Venkateshwarulu, AK Shanker, C Shanker, M Maheswari (eds.). Springer Science Business Media BV.

Prasannakumar, N. R. & Subhash Chander & R. N. Sahoo. (2014). Characterization of brown planthopper damage on rice crops through hyperspectral remote sensing under field conditions. Phytoparasitica ISSN 0334-2123 Vol 42 Number 3 Phytoparasitica (2014) 42:387-395

Savary S., Ficke A., Aubertot J., Hollier C., (2012). Crop losses due to diseases and their implications for global food production losses and food security. Food Secure. 2012; 4:519–537.

Savary S., Willocquet L., Pethybridge S.J., Esker P., McRoberts N., and Nelson A. (2019) The global burden of pathogens and pests on major food crops. Nature Ecology and Evolution 4, 430-439.

Singh B, Singh M, Singh G, Suri K, P.P.S. Pannu and S.K. Bal. (2012). Hyperspectral data for the detection of rice bacterial leaf blight (blb) disease. Proceedings of Agro-Informatics and Precision Agriculture (AIPA) 2012

Subbarao, B.L., Ghosh, A., John, V.T., (1979). Effect of rice tungro virus on chlorophyll and anthocyanin pigments in two rice cultivars. J. Phytopathol. 94, 367–371.

Weisstein, Eric W. "Bonferroni Correction." From MathWorld--A Wolfram Web Resource. http://mathworld.wolfram.com/BonferroniCorrection.html

Yuan, L., Huang, Y., Loraamm, R. W., Nie, C., Wang, J., & Zhang, J. (2014). Spectral analysis of winter wheat leaves for detection and differentiation of diseases and insects. Field Crops Research, 156, 199–207. doi: 10.1016/j.fcr.2013.11.012

Zhang, J.C., Pu, R.L., Huang, W.J., Luo, J.H., Wang, J.H., (2012). Using in-situ hyperspectral data for detecting and discriminating yellow rust disease from nutrient stresses. Field Crops Research 134, 165–174.